Hydrogen Exchange

DOI: 10.1002/anie.201206828

Rapid Characterization of Hydrogen Exchange in Proteins**

Anushikha Thakur, Kousik Chandra, Abhinav Dubey, Patrick D'Silva, and Hanudatta S. Atreya**

The study of structure, folding, and dynamics in proteins is assisted by the elucidation of kinetics and thermodynamics of the hydrogen–deuterium exchange.[1,2] The kinetics of the process is characterized by measurement of amide hydrogen exchange rates,[2,3] whereas the protium–deuterium fractionation factor, which is based on the equilibrium of the exchange process, helps to understand the thermodynamic aspects and the strength of hydrogen bonds.[4–9] Using NMR spectroscopy, slow amide hydrogen exchange rates ($k_{ex} < 1\,s^{-1}$) are generally measured by monitoring the time-dependent change in intensity of the signals of amide protons upon dissolution of the protein in ^2H_2O. Measurement of fast exchange rates, however, remains a challenge.[10–14] On the other hand, to measure the protium–deuterium fractionation factors, a series of two-dimensional (2D) experiments are usually performed with different protein samples dissolved in varying molar ratios of H_2O:^2H_2O.[4,8,9] We describe here a simple NMR method to elucidate both hydrogen–deuterium fractionation factors and fast hydrogen exchange with a single type of experiment. The method is based on the 2D ^{13}CO–^{15}N correlation experiment (2D-CON)[15] involving ^{13}C detection, which has high resolution and sensitivity and can be acquired rapidly. The method is illustrated on three proteins with one of them being intrinsically disordered, as it has amide protons that span a wide range of exchange rates.

The key idea is to detect simultaneously and in a well-resolved manner the signals of deuterated (ND) and non-deuterated (NH) amides such that their intensities and exchange between the two sites can be measured. This is achieved by acquiring the 2D-CON spectrum on a ^{13}C,^{15}N-labeled protein that is dissolved in a mixture of H_2O:^2H_2O. In such a sample, the ND species (hereafter referred to as CO-ND) gets separated from the NH (CO-NH) in both F1 and F2 dimension of the 2D spectrum because of two-bond ($^2\Delta^{13}CO(D)$) and one-bond ($^1\Delta^{15}N(D)$) deuterium isotope effect on ^{13}CO and ^{15}N shifts, respectively (Figure 1). Typically, the $^2\Delta^{13}CO(D)$ and $^1\Delta^{15}N(D)$ have a value of around 0.08 ppm[7,16] and around 0.75 ppm,[17] respectively. A separation (Δ) of approximately 50 Hz is thus obtained between CO-NH and CO-ND peaks at a field strength of 16.4 T (^1H resonance frequency of 700 MHz) used in this study. The exchange of magnetization between the two species is characterized by two-site exchange.[18] The separation and thereby the range of exchange rates, k_{ex}, accessible increases with the field strength.

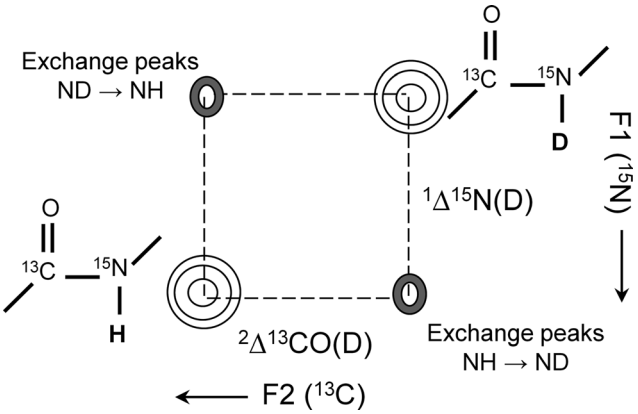

Figure 1. Schematic illustration of the peak pattern observed in 2D-^{13}CO–^{15}N acquired for a protein dissolved in a 1:1 mixture of H_2O:^2H_2O. The exchange peaks shown are observed in 2D-CON-EXSY (see text), which employs heteronuclear ZZ-exchange spectroscopy to monitor exchange of magnetization between CO-NH and CO-ND.

A wide range of exchange rates can be measured using this approach. First, in the case of $k_{ex} > (\pi\Delta/\sqrt{2})$ (corresponding to $\approx 100\,s^{-1}$ at 16.4 T), the two peaks start to coalesce and exchange rates can be estimated based on their linewidths in the ^{15}N dimension. This estimation is achieved by comparing the linewidths with that measured in the sample prepared in 100 % H_2O (which represents the case of no exchange).[16] The difference in ^{15}N linewidths for a residue between the two samples can be used for measuring the exchange rates, assuming a two-state exchange model.[18] Second, for residues having $k_{ex} < (\pi\Delta/\sqrt{2})$, the $^{13}CO_{i-1}$–$^{15}N_i$ cross-peaks corresponding to CO-NH and CO-ND get resolved in F1 and F2 dimensions (Figure 1). In such cases, heteronuclear ZZ-exchange spectroscopy[19] is employed (described below) and the exchange of heteronuclear longitudinal two-spin order ($2C'_ZN_Z$) between CO-NH and CO-ND species is

[*] A. Thakur,[+] Dr. K. Chandra,[+] A. Dubey, Prof. H. S. Atreya
NMR Research Centre, Indian Institute of Science
Bangalore-560012 (India)
E-mail: hsatreya@sif.iisc.ernet.in
Homepage: http://nrc.iisc.ernet.in/hsa
A. Thakur,[+] Dr. P. D'Silva
Department of Biochemistry, Indian Institute of Science
Bangalore-560012 (India)
E-mail: patrick@biochem.iisc.ernet.in
[+] These authors contributed equally to this work.

[**] H.S.A. acknowledges research support from DAE, DST, and DBT research grants. P.D.S. acknowledges support from Wellcome Trust International Senior Research Fellowship in Biomedical Science (UK), WT081643MA. We thank Dr. John Cort, PNNL, for providing the ubiquitin plasmid and Garima Jaipuria, IISc, for help in recording NMR spectra.

Supporting information for this article is available on the WWW under http://dx.doi.org/10.1002/anie.201206828.

monitored as a function of time. Third, for slow exchange rates ($k_{ex} < 1\ s^{-1}$), the increase in intensity of the CO-ND cross-peak as a function of time is monitored immediately upon dissolution of the protein (lyophilized in H_2O) in a mixture of H_2O:^2H_2O.

Using the same sample and spectrum acquired for measuring exchange rates, the protium–deuterium fractionation factor (ϕ) can be measured. The ratio of intensities of the two cross-peaks corresponding to the CO-NH and CO-ND gives ϕ.[7] The CO-NH and CO-ND species have different relaxation rates because of the differential interaction of ^{13}CO and ^{15}N with ^1H versus ^2H (described in detail in the Supporting Information). Hence, a correction factor is needed when measuring ϕ to account for the difference in the intensities of the isotope-shifted peaks.

Figure 2a shows a selected region of the 2D-CON spectrum acquired for the intermembrane space region of TIM23 from *S. Cerevisiae* (TIM23-IMS; 12 kDa), an essential component of the mitochondrial protein translocation machinery.[20] Most of the residues in TIM23-IMS (which is intrinsically disordered) are well resolved and show the two diagonally separated CO-NH and CO-ND peaks. The measured fractionation factors are tabulated in Section S5 of the Supporting Information. In certain cases, there is an ambiguity in identifying the correct CO-ND partner for a given CO-NH peak (e.g., for L35 shown in Figure 2b). This ambiguity can be resolved using a modified version of 2D-CON designed to selectively detect CO-NH and CO-ND cross-peaks in separate spectra (the radio frequency (r.f.) pulse scheme is shown in Figure S3). The selectivity is based on exploiting the one-bond J-coupling between ^{15}N and HN that is present in the CO–NH species and absent in the CO–ND species. The two peaks (corresponding to CO–NH and CO–ND) in 2D-CON are thus separated into different spectra (shown overlayed in Figure 2c).

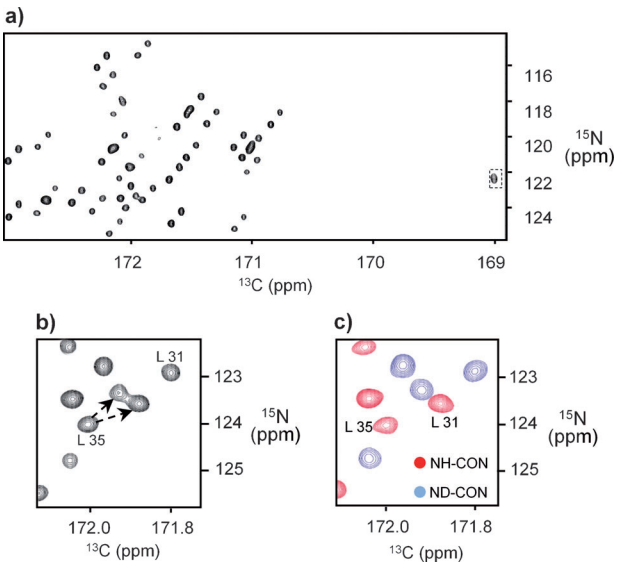

Figure 2. a) A region of 2D-CON spectrum acquired for TIM23-IMS in a 1:1 mixture of H_2O:^2H_2O. b) A region of 2D-CON depicting the ambiguity in assigning the CO-ND partner for a given CO-NH peak. This ambiguity is resolved by acquiring separately NH- and ND-selective 2D-CON (overlayed in (c)). The spectra were acquired at 16.4 T and 25 °C with samples with a concentration of 0.7 mM and a measurement time of 1.3 h.

In the case of fast exchange ($k_{ex} > 100\ s^{-1}$ at 16.4 T), a singlet is observed in the 2D-CON because of coalescence (Figure 3). Correspondingly, a peak at the same chemical shifts as the singlet is observed in each of NH- and ND-selective 2D-CON spectra. In TIM23-IMS, Arg91 (the peak of which is shown in dotted box in Figure 2a) gives a singlet at 298 K implying $k_{ex} \gg 100\ s^{-1}$ (Figure 3). At lower temperatures, the NH and ND cross-peaks begin to resolve, thus indicating a slowing down of exchange. By measuring ^{15}N linewidths in samples prepared in a 1:1 mixture of H_2O:^2H_2O and 100% H_2O (representing no-exchange) and assuming a two-site exchange,[18] a k_{ex} of approximately $300\ s^{-1}$ was estimated at 308 K. A similar case was observed in another protein that involves the N-terminal residue of human J-protein co-chaperone ($Dph4_{93-149}$;[21] Figure S7). Because of the difference in relaxation rates of CO-NH and CO-ND, as mentioned above, an average linewidth of 12 Hz and 8 Hz, respectively, was observed for TIM23-IMS. Thus, an average of two linewidths was used to estimate the exchange rates.

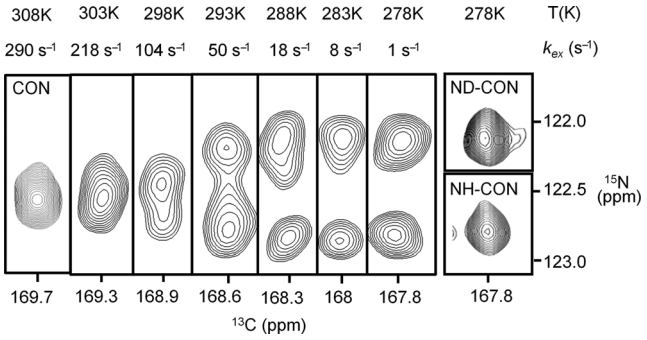

Figure 3. The ^{13}CO–^{15}N cross-peak for Arg91 of TIM23-IMS, acquired in a 1:1 mixture of H_2O:^2H_2O. The exchange rates measured from ^{15}N linewidths at different temperatures are indicated. The two peaks observed at lower temperatures correspond to CO-NH and CO-ND, as verified by acquiring a NH- and ND-selective 2D-CON shown on the extreme right. Spectra were acquired with samples with a concentration of 0.7 mM (TIM23) and a measurement time of 1.3 h (Table S1).

For measuring of amide hydrogen exchange rates in the range 1–15 s^{-1}, a slightly modified version of 2D-CON (referred to as 2D-CON-EXSY; Figure S3) was developed to monitor the exchange of heteronuclear longitudinal two-spin order ($2C'_zN_z$) between the CO-NH and CO-ND species as a function of time. Figure 4a illustrates the peak pattern observed for some residues in TIM23-IMS dissolved in a 1:1 mixture of H_2O:^2H_2O. The exchange rates can be estimated by fitting the intensity of exchange peaks to the following equation (Figure 4b; τ_m is the mixing time) assuming two-site exchange:[18]

$$I_{\text{exchange-peak}} = I_0\left(1 - e^{-k_{ex}\cdot\tau_m}\right)\left(e^{-R_1\cdot\tau_m}\right) \quad (1)$$

Here, I_0 represents the population of CO-NH/CO-ND species, and $R_1 \approx 1.5\ s^{-1}$ the relaxation rate of $2C'_zN_Z$ (an

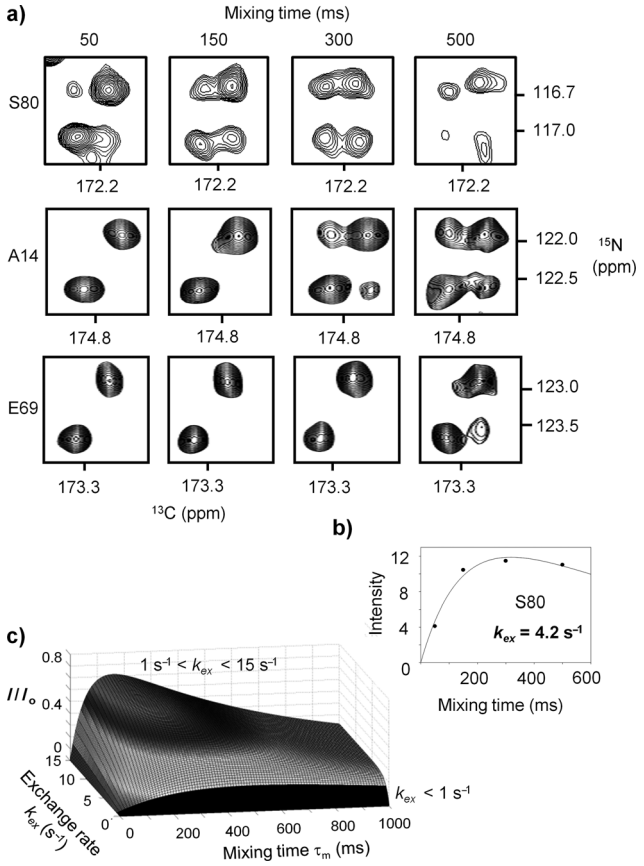

Figure 4. a) Illustration of the peak pattern observed in 2D-CON-EXSY spectrum of TIM23-IMS at different mixing times (indicated at the top). Selected residues are shown which have different exchange rates. b) A plot of the intensity of the exchange peak for S80 as a function of mixing time. The exchange rate was estimated using Equation (1). c) Surface plot depicting the variation of the intensity of exchange peaks [I/I_0 in Eq. (1)] as a function of exchange rates and mixing time. Two regions are indicated: $k_{ex} < 1\ s^{-1}$ and $1 < k_{ex} < 15\ s^{-1}$. The 2D-CON-EXSY spectra were acquired at 25 °C with a sample of TIM23-IMS (0.7 mM) and a measurement time of 1.1 h (Table S1).

average of $2C'_ZN_Z$ (H) and $2C'_ZN_Z$(D)) for proteins used in the present study (Section S6 of the Supporting Information).

Qualitatively, using mixing times in the range of 0–500 ms, two exchange regimes can be broadly identified. This result is based on the assumption that for the exchange peak to be observed, its intensity should be significant (>10% of the diagonal).[22] For instance, residues that start to show strong exchange peaks at a mixing time (τ_m) of 50–150 ms (Figure 4c) will typically have $k_{ex} = 1$–$15\ s^{-1}$, whereas those that have significantly strong exchange peaks starting only from $\tau_m = 300$–500 ms will have $k_{ex} < 1\ s^{-1}$. For $k_{ex} > 15\ s^{-1}$, exchange peaks begin to overlap with the originating peaks in F2 (^{13}C) because of broadening of lines, thus rendering the measurement of exchange rates difficult for higher k_{ex} values.

Using 2D-CON and 2D-CON-EXSY as described above, residues with different exchange regimes were elucidated in TIM23-IMS (Figure 5a). It is interesting to note that the protein, even though intrinsically disordered, has residues with exchange rates ranging from slow to very fast. In

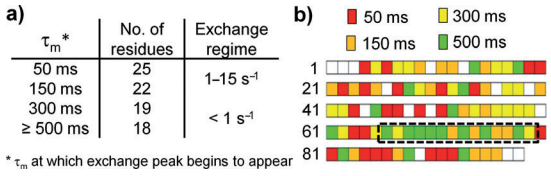

Figure 5. a) The number of residues in TIM23-IMS which show exchange peaks in 2D-CON-EXSY, starting at different mixing time. b) Residues in TIM23-IMS exhibiting different exchange regimes indicated by different color codes. Residues shown in dotted box are contiguous residues with slow exchange rates and are close to the binding site where the incoming precursor proteins bind TIM23-IMS.

particular, a contiguous segment of residues 66–79 exhibit slower exchange rates (shown in dotted box in Figure 5b). This result could be due to the fact that this region is close to the putative site where the incoming precursor proteins bind TIM23-IMS in association with other components of the presequence translocases.[20]

In the case of structured proteins, slow exchange and/or stronger hydrogen bonds result in weaker CO-ND cross-peaks compared to those of CO-NH.[4] For amides that have very slow exchange rates ($k_{ex} < 0.1\ s^{-1}$), upon dissolution of the protein in a 1:1 mixture of H_2O:^2H_2O, the CO-ND peaks are initially absent, and their intensity increases with time until an equilibrium is reached. This observation is exemplified for ubiquitin (Figure 6a). The protein sample was lyophilized in H_2O and dissolved in a 1:1 mixture of H_2O:^2H_2O. For some of the amides with slow exchange rates (shown in dotted box), the CO-ND peaks are absent, indicating that the amide groups have not exchanged sufficiently with ^2H_2O. This result is further verified by recording the NH- and ND-selective 2D-CON, which con-

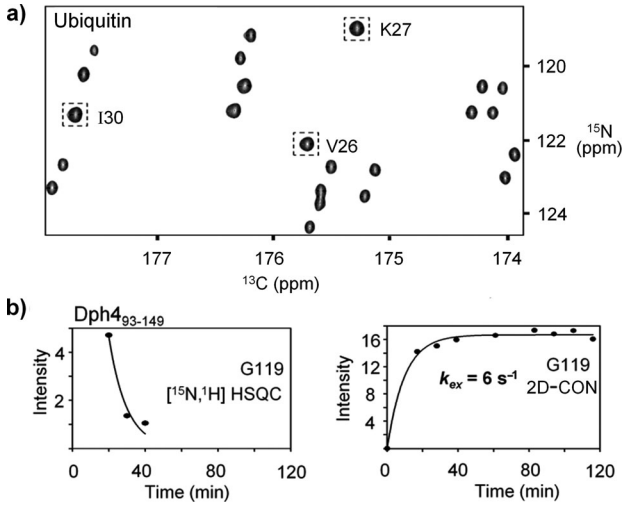

Figure 6. Selected region from a) 2D-CON and b) 2D-NH- and ND-CON spectrum of ubiquitin showing residues (boxed) that lack CO-ND peaks because of very slow exchange (also depicted in Figure S8). b) Intensity plots of amide proton signal of G119 (Dph4$_{93-149}$) upon dissolution of protein in ^2H_2O in 2D [^{15}N–^{1}H] HSQC (left) and 2D-ND-CON (right) at different times. Spectra were acquired on ubiquitin (1 mM) and Dph4$_{93-149}$ (around 0.8 mM) samples with measurement times of 20 min (for a) and 8 min (for b; Table S1).

firms that a CO-ND peak is indeed absent initially and appears slowly with time for some residues (Figure S8). In 2D-CON-EXSY, most of the residues do not show an exchange peak, even at $\tau_m = 500$ ms at 313 K (Figure S9), thus implying very slow exchange.[23]

By lyophilizing the protein in H_2O followed by dissolution in 100% ^2H_2O, the increase in intensity of CO-ND peaks as a function of time can be used to measure exchange rates that otherwise are too fast to be measured from a 2D [^{15}N–^{1}H] HSQC. In 2D [^{15}N–^{1}H] HSQC, the initial intensity of amide protons is lost quickly because of the delay of the experiment, whereas in a series of 2D-CON acquired, the intensity of the CO–ND peak can be considered as zero at $t = 0$, which helps in calculating exchange rates. This is exemplified for Gly119 of $Dph4_{93-149}$, for which the amide exchange rate could not be measured from 2D [^{15}N–^{1}H] HSQC (Figure 6b, left) because of a rapid decrease in intensity with time. However, the exchange rate could be measured from the intensity of the CO-ND peak in the ND-selective 2D-CON as a function of time (Figure 6b, right).

In summary, Table 1 depicts the different exchange regimes that can be elucidated using the approach described above. The 2D-^{13}CO–^{15}N and its variants presented herein provide key advancements over earlier methods for measuring fractionation factors[4,7–9] and amide exchange rates.[10,12] 1) All parameters are obtained from a single type of experiment, thus facilitating rapid analysis. 2) A 2D-CON has good dispersion and resolution (illustrated in Figure S12 in the Supporting Information) and is useful particularly for structurally disordered systems.[24] (The estimate of signal-to-noise ratio (S/N) as a function of rotational correlation time is shown in Figure S13. Note that for proteins with small molecular weight, higher sensitivity can be obtained using ^{13}C-detected 2D-(HACA)CON, in which the polarization starts from $^1H^\alpha$ (Figure S4 and S10).) 3) Intensities of the peaks are not affected by the longitudinal relaxation of amide protons and their interaction with other protons and solvent magnetization (by exchange/NOE), which has to be considered in ^{1}HN-detected experiments. 4) The separation between CO-NH and CO-ND peaks and thereby the range of exchange rates (k_{ex}) accessible increases with field strength. 5) The smaller $^2\Delta^{13}$CO(D) is detected in the direct dimension in contrast to their detection in the indirect dimension[7] which warrants long measurement times to obtain sufficient resolution. A method that involves the detection of ^{13}CO-H and ^{13}CO-D for measuring amide exchange rates has been proposed.[16] The method is however a 1D approach that is limited by the smaller separation between ^{13}CO-H and ^{13}CO-D compared to ^{15}N–H and ^{15}N–D. The method presented herein thus has a range of applications, such as in protein-folding and ligand-binding studies to monitor structural/dynamic changes, and can be used in conjunction with the recently developed techniques for measuring very fast proton exchange rates.[14]

Table 1: Exchange rates measurable from 2D-CON (at 16.4 T).

Method	Exchange rates
^{15}N linewidths[a]	$1\ s^{-1} < k_{ex} < 1000\ s^{-1}$
2D-CON-EXSY	$1\ s^{-1} < k_{ex} < 15\ s^{-1}$
Intensity build up	$k_{ex} < 1\ s^{-1}$

[a] Together with ^{15}N linewidths measured in sample prepared in 100% H_2O.

Received: August 23, 2012
Revised: November 3, 2012
Published online: January 22, 2013

Keywords: amides · fractionation factors · hydrogen exchange · protein folding

[1] S. W. Englander, L. Mayne, *Annu. Rev. Biophys. Biomol. Struct.* **1992**, *21*, 243.
[2] C. M. Dobson, P. J. Hore, *Nat. Struct. Mol. Biol.* **1998**, *5*, 504.
[3] Y. Bai, T. R. Sosnick, L. Mayne, S. W. Englander, *Science* **1995**, *269*, 192.
[4] S. N. Loh, J. L. Markley, *Biochemistry* **1994**, *33*, 1029.
[5] A. S. Edison, F. Weinhold, J. L. Markley, *J. Am. Chem. Soc.* **1995**, *117*, 9619.
[6] B. A. Krantz, L. B. Moran, A. Kentsis, T. R. Sosnick, *Nat. Struct. Mol. Biol.* **2000**, *7*, 62.
[7] A. C. LiWang, A. Bax, *J. Am. Chem. Soc.* **1996**, *118*, 12864.
[8] G. Veglia, A. C. Zeri, C. Ma, S. Opella, *Biophys. J.* **2002**, *82*, 2176.
[9] D. Khare, P. Alexandr, J. Orban, *Biochemistry* **1999**, *38*, 3918.
[10] G. Gemmecker, W. Jahnke, H. Kessler, *J. Am. Chem. Soc.* **1993**, *115*, 11620.
[11] T. L. Hwang, P. C. M. van Zijl, S. Mori, *J. Biomol. NMR* **1998**, *11*, 221.
[12] T. Brand, E. J. Cabrita, G. A. Morris, R. Gunther, H. J. Hofmann, S. Berger, *J. Magn. Reson.* **2007**, *187*, 97.
[13] S. Koide, W. Jahnke, P. E. Wright, *J. Biomol. NMR* **1995**, *6*, 306.
[14] a) T. Segawa, F. Kateb, L. Duma, G. Bodenhausen, P. Pelupessy, *ChemBioChem* **2008**, *9*, 537; b) F. Kateb, P. Pelupessy, G. Bodenhausen, *J. Magn. Reson.* **2007**, *184*, 108.
[15] W. Bermel, I. Bertini, L. Duma, I. C. Felli, L. Emsley, R. Pierattelli, P. R. Vasos, *Angew. Chem.* **2005**, *117*, 3149; *Angew. Chem. Int. Ed.* **2005**, *44*, 3089.
[16] G. D. Henry, J. H. Weiner, B. D. Sykes, *Biochemistry* **1987**, *26*, 3626.
[17] J. Abildgaard, P. E. Hansen, M. N. Manalo, A. Liwang, *J. Biomol. NMR* **2009**, *44*, 119.
[18] a) H. M. McConnell, *J. Chem. Phys.* **1958**, *28*, 430; b) J. Jeener, B. H. Meier, P. Bachmann, R. R. Ernst, *J. Chem. Phys.* **1979**, *71*, 4546.
[19] G. Montelione, G. Wagner, *J. Am. Chem. Soc.* **1989**, *111*, 3096.
[20] L. De La Cruz, R. Bajaj, S. Becker, M. Zweckstetter, *Protein Sci.* **2010**, *19*, 2045.
[21] A. Thakur, B. Chitoor, A. V. Goswami, G. Pareek, H. S. Atreya, P. D'Silva, *J. Biol. Chem.* **2012**, *287*, 13194.
[22] P. Wenter, G. Bodenhausen, J. Dittmer, S. Pitsch, *J. Am. Chem. Soc.* **2006**, *128*, 7579.
[23] C. Bougault, L. Feng, J. Glushka, E. Kupce, J. H. Prestegard, *J. Biomol. NMR* **2004**, *28*, 385.
[24] V. Csizmok, I. Felli, P. Tompa, L. Banci, I. Bertini, *J. Am. Chem. Soc.* **2008**, *130*, 16873–16897.

